CFD analysis of solar air heater having absorber plate roughened with compound turbulators

[1]Mr. Obaid Ul Haque Ansari,[2]Dr. V.R. Kalamkar,
[1]PG Student,[2]Associate Professor
[1]Department of Mechanical engineering,
[1]Visvesvaraya National Institute of Technology , Nagpur, India

***Abstract*—In the present work the thermo hydraulic performance of solar air heater having absorber plate roughened with compound turbulators is analyzed using Computational Fluid Dynamics (CFD). The effect of absorber plate geometry on heat transfer and friction factor is studied by varying the relative roughness height (e/D_H) from 0.025 to 0.040(4 values) and relative roughness pitch (P/e) from 8 to 15 (4 values). Range of Reynolds number selected for numerical simulation is 3000 to 18,000 (6 values). Different turbulent models have been used for the analysis of solar air heater and their results are compared with the experimental data available in the literature. The results obtained using K-ϵ Standard model have been found in good agreement with the experimental results and hence this model is used to predict the heat transfer and friction factor in the roughened duct for various geometries of an absorber plate. The thermo hydraulic performance parameter (THPP) is also evaluated for each plate to predict the overall performance and also for selecting the best geometry for the range of parameter investigated.**

IndexTerms—**Solar Air Heater, Heat Transfer, Friction Factor, Compound Turbulators, Thermo Hydraulic Performance Parameters (THPP)**.

I. INTRODUCTION

The demand of the energy is increasing day by day on the other hand the fossil fuels are depleting continuously and rapidly. This leads to the continuous increase in demand supply energy gap. In order to fulfill this huge energy gap, lots of research is going on all around the world to utilize the renewable sources of energy properly and efficiently. Among all the renewable sources of energy Solar energy is available in plenty as compared to other renewable sources of energy like wind energy, tidal energy, ocean energy, wave energy, geothermal energy etc. This solar energy can be properly utilized by converting it first into thermal energy using solar collectors and then using this energy in various applications.

Among the various solar collector systems solar air heater is the simplest and cheapest way to convert the solar energy into thermal energy. It has various advantages like compact and less complicated system, it can be design using cheaper and lesser material as compared to solar water heater and best part is air ass working fluid which is non-toxic, freely available, corrosion free, its leakage doesn't harm the environment etc. It has variety of applications like space heating for residential and commercial applications, drying of laundry, agricultural crops (i.e. tea, corn, and coffee) and other drying applications, seasoning of wood etc. But poor thermal conductivity of air leads to lesser heat transfer coefficient between absorber plate and air which leads to poor performance of solar air heater. In order to enhance this performance, a passive technique of introducing artificial roughness in absorber plate is the most common technique trending nowadays. Use of artificial roughness creates turbulence inside the duct which effectively increases the heat transfer rate and on the contrary it also increases the friction factor which leads to high pumping power. So to avoid higher requirement of pumping power turbulence must be created only near to absorber plate (i.e. in laminar sub layer zone only).

Lots of research has been carried out by various investigators experimentally as well as numerically in order to predict the performance of solar air heater with artificial roughness on absorber plate. Summary of various numerical and theoretical studies has been discussed in the review papers [1-4]. The number of numerical studies reported is quite less compared to the number of experimental studies. Bhagoria et al. [5] have performed experimental investigation of solar air heater with wedge shaped roughness element. By varying the rib height, pitch and wedge angle 20 different absorber plate geometries have obtained and analysed in order to optimize these parameters. Correlations for Nusselt number and friction factor has also been developed by them. The maximum enhancement of heat transfer is occurred corresponding to wedge angle (Φ) =10^0. Chaube et al. [6] numerically investigated heat transfer and flow characteristics for a duct having roughness element in the form of transverse rectangular ribs. They have carried out numerical analysis using SST k-ω model which are in good agreement with the experimental results. The analysis reveals that maximum local heat transfer coefficient occurs at the point of reattachment. Aharwal et al. [7] have performed experimental investigation on repeated inclined square cross sectioned ribs with gap. The angle of attack (α) has been kept constant = 60^0 for the study and the variation in performance with relative gap width (g/e) and relative gap position (d/W) is analysed. The THPP is found to be the maximum for the relative gap width of 1.0 and the relative gap position of 0.25. Saini and Saini [8] have carried out experimental investigation on solar air heater with artificial roughness in the form of arc shaped wires. They have studied the effect of variation of relative roughness height and relative arc angle (α/90) on performance of solar air heater. Using the experimental results the correlations for Nusselt number and friction factor has also been developed which gives good agreement between predicted and experimental values. Kumar et al. [9] have carried out experimental

investigation to study heat transfer and fluid flow characteristics of solar air heater with discrete W- shaped ribs as roughness element. The relative roughness pitch (P/e) is kept constant = 10 for the study while the relative roughness height (e/D_H) and angle of attack (α) is varied (30^0 to 75^0) to obtain 20 different geometries of roughened duct. They have also develop the correlations for Nusselt Number and friction factor and the maximum value of both Nusselt number and friction factor is found to be maximum corresponding to angle of attack (α) = 60^0. Lanjewar et al [10] have performed experimental investigation of solar air heater with different orientations of W-shaped ribs (W-up and W- down) as roughness elements. W-up and W- down represents W pointing towards upstream and downstream respectively. It has observed that W-down ribs give better THPP than W-up and V-ribs. Maximum THPP for W-down ribs is 1.98 while it is 1.81 for W-up ribs in the range of parameters investigated. Lanjewar et al [11] have carried out experimental investigation to study heat transfer and fluid flow characteristics of solar air heater with discrete W-shaped ribs as roughness element. The relative roughness pitch (P/e) is kept constant = 10 for the study while the relative roughness height (e/D_H) and angle of attack (α) is varied (30^0 to 75^0). They have also develop the correlations for Nusselt Number and friction factor and the maximum thermo hydraulic performance parameter is found to be maximum corresponding to angle of attack (α) = 60^0. Kumar et al [12] have carried out experimental investigation of heat transfer and fluid flow in solar air heater with multi v-shaped ribs with gap roughness on absorber plate. Various roughness parameters like relative gap distance (Gd/Lv) of, relative gap width (g/e) are varied while some parameters like relative width ratio (W/w) = 6 relative roughness height (e/D) = 0.043, relative roughness pitch (P/e) = 10 and angle of attack (α) of 60^0 are kept constant. It is observed presence of gap in multi v- shaped ribs considerably increases the heat transfer considerably. The maximum values of Nusselt number and friction factor is obtained for relative gap distance of 0.69 and a relative gap width of 1. Also it has been concluded that Multi v-rib with gap roughness is thermo hydraulically better in comparison to inclined rib with gap, v-rib, broken inclined rib and multi v-rib without gap. Kumar and Saini [13] carried out numerical study to the effect of arc shaped geometry on thermal, hydraulic and overall performance of solar air heater. Thin circular wire of arc shape is used as roughness element. Karmare and Tikekar [14] have employed metal ribs of circular, square and rectangular cross section at an inclination of 60° to the direction of air flow. The rib elements are arranged in the form of staggered grit and optimization of rib geometry and angle of attack is carried out using CFD tool. Yadav and Bhagoria [15-17] have performed numerical investigations to study the effect of introducing artificial roughness in the form of transverse ribs of circular, square and triangular cross section. They have used RNG k-ε turbulence model to simulate the flow through the roughened duct for all geometries. The results of their studies reveal that for all the roughness geometries the Nusselt number increases with increase in relative roughness height where as it decreases with increase in relative roughness pitch. Boukadoum and Benzaoui [18] have performed CFD simulation to analyse the heat transfer and flow along the solar air heater duct provided with transverse rectangular ribs. They used RANS formulation to model the flow. They have found that K-ω SST model gives the best results close to the experimental results available. Jin et al. [19] carried out 3D numerical investigation of heat transfer and fluid flow in solar air heater with multi v- shaped ribs on absorber plate. The simulations are performed for different rib geometries with a varying span wise V-rib number, relative rib pitch, relative rib height, and angle of attack for different Reynolds numbers. The effect of these parameters on Nusselt number, friction factor and flow pattern is analysed and it is observer that multi v- ribs effectively increases the heat transfer and overall performance of solar air heater. The maximum THPP was found to be 1.93 for the range of roughness parameters investigated. Layek et al [20] have employed compound turbulators (chamfered ribs with 60° V-grooves), to improve the performance of solar air heaters. They have started the experimental investigation by 0° chamfered ribs (square ribs) and then they had varied the chamfer angle to 5°, 12°, 15°, 18°, 22° and 30^0 without any change in other parameters like relative roughness height (e/D_H = 0.030), relative roughness pitch (P/e = 10), relative groove position (g/P = 0.5) etc. Hence the effect of chamfering on the solar air heater with compound turbulators is studied to find out the optimum chamfer angle which comes out to be 18°. In the present investigation instead of studying the effect of chamfering the relative roughness height and relative roughness pitch is varied while relative groove position is kept same (g/P =0.5). By taking relative roughness height as e/D_H = 0.025,0.030,0.035 and 0.040 and relative roughness pitch as P/e = 8, 10, 12 and 15, sixteen different 2D geometries has been created in ICEM 16.0 and simulated using FLUENT 16.0 solver. The depth of the 60° V-grooves is kept equal to height of the square rib in each case. The duct width, height and aspect ratio is same for previous experimental investigation conducted by Layek et al [20] and current numerical investigation. The result available from experimental investigation of 0° chamfer ribs (square ribs) is used for the validation of current numerical investigation..

II. ANALYSIS

A. Computational Domain

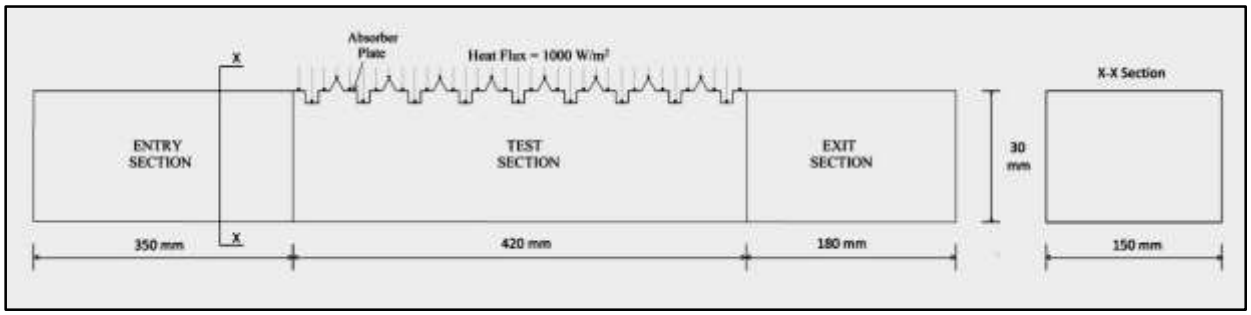

figure 1: schematic of 2D computational domain

Figure 1 shows schematic of computational domain considered for the CFD analysis. It is also the computational domian for the current analysis. The height(H) and width(W) of the duct is taken as 30 mm and 150 mm respectively so that aspect ratio (W/H) can be maintained equal to 5. The entry section and exit section are provided to reduce the end effect. The length of the entry section, test section and exit section is taken as 350mm , 420 mm and 180 mm respectively based on ASHRAE recommendations [21]. A constant heat flux of 1000 W/m^2 is considered for the analysis which is equivalent to the average solar irradiation. All the other walls of the duct are made insulated.

B. Roughness Geometry and Range of Roughness Parameters

The geometry of the roughened duct is shown in Figure 2.The relative roughness height and relative roughness pitch is varied while relative groove position is kept same (g/P = 0.5) for each case. Also the depth of the 60° V-grooves is kept equal to height of the square rib in each case. By taking relative roughness height as e/D_H = 0.025, 0.030, 0.035 and 0.040 and relative roughness pitch as P/e = 8, 10, 12 and 15, sixteen different 2D geometries and their created in ANSYS ICEM 16.0.

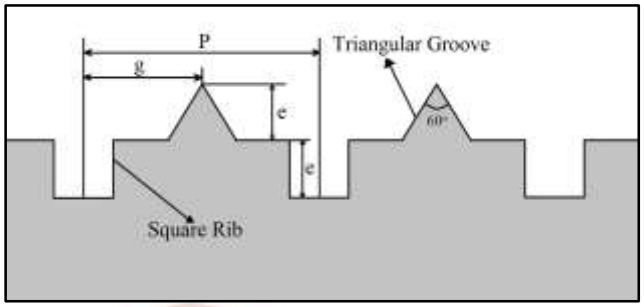

figure 2: roughness geometry

The various parameters of all sixteen absorber plate geometries are summarized in Table 1.

table 1: range of roughness parameters

	RIB HEIGHT (e), mm	RELATIVE GROOVE POSITION (g/P)	RELATIVE ROUGHNESS PITCH (P/e)	RELATIVE ROUGHNESS HEIGHT (e/D_H)	PITCH (P), mm	NO. OF RIBS
Plate 1	1.25	0.5	8	0.025	10.00	41
Plate 2	1.25	0.5	10	0.025	12.50	33
Plate 3	1.25	0.5	12	0.025	15.00	27
Plate 4	1.25	0.5	15	0.025	18.75	22
Plate 5	1.50	0.5	8	0.030	12.00	34
Plate 6	1.50	0.5	10	0.030	15.00	27
Plate 7	1.50	0.5	12	0.030	18.00	23
Plate 8	1.50	0.5	15	0.030	22.50	18
Plate 9	1.75	0.5	8	0.035	14.00	29
Plate 10	1.75	0.5	10	0.035	17.50	23
Plate 11	1.75	0.5	12	0.035	21.00	19
Plate 12	1.75	0.5	15	0.035	26.25	15
Plate 13	2.00	0.5	8	0.040	16.00	26
Plate 14	2.00	0.5	10	0.040	20.00	20
Plate 15	2.00	0.5	12	0.040	24.00	17
Plate 16	2.00	0.5	15	0.040	30.00	13

C. Mesh Generation

Analysis is carried out for all the sixteen roughened duct geometries for Re = 3000, 6000, 9000, 12000, 15000 and 18000. Fine meshing is provided near all the walls in order to efficiently capture the boundary layer phenomena as shown in Figure 3. Using the properties of air mentioned in Table 2 the distance of first node from the wall is estimated using Y+ calculator from www.cfd-online.com/Tools/yplus.php [22] for Y+ < 2. This distance also depends on the operating velocity (Reynolds Number). Hence the grid will vary not only with the variation in roughness geometry but also vary with the change in velocity for the same roughned duct. Hence in total 96 (16*6) different mesh are created in ANSYS ICEM 16.0. In each mesh the maximum cell size is kept = 0.3 mm. Hence the no. of nodes for each mesh will differ depending upon roughness geometry and operating velocity.

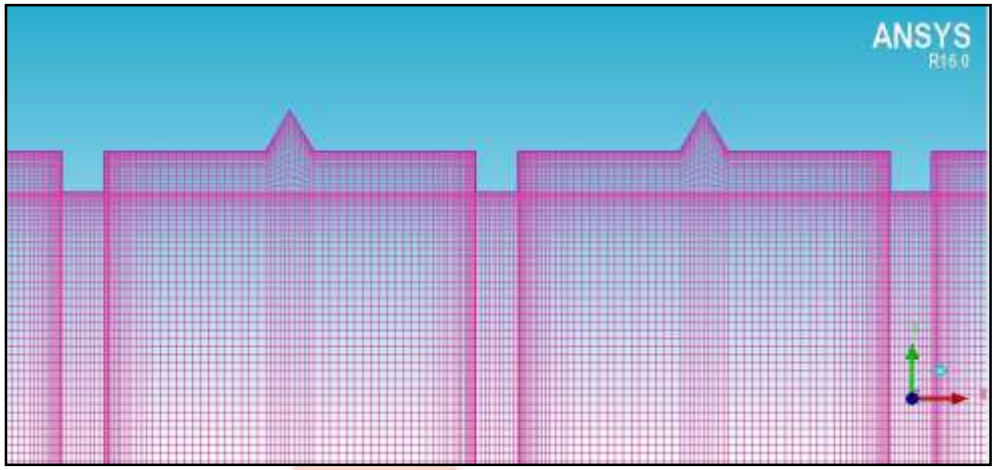

figure 3: 2D structured meshing

table 2: standard properties of material

	MATERIAL	PROPERTIES
WORKING MEDIUM	Air	Density, ρ = 1.225 Kg/m^3 Specific Heat, C_p = 1006.43 J/Kg-K Thermal Conductivity, K = 0.0242 W/m-K Dynamic Viscosity, μ = 1.7894*10^{-5} Kg/m-s
ABSORBER PLATE	Aluminum	Density, ρ = 2719 Kg/m^3 Specific Heat, C_p = 871 J/Kg-K Thermal Conductivity, K = 202.4 W/m-K

D. CFD Analysis

The investigation of heat transfer and fluid flow phenomena through the artificially roughened solar air heater is carried out using 2D Numerical model. Since the geometry is simple and ribs are transverse, 2D numerical model will be sufficient for analysis of flow through the duct as it will same computational power and computational time. ANSYS FLUENT 16.0 is the code used for solving the continuity, momentum and energy equations. The present CFD simulation is carried out under the following assumptions

1. The flow is 2D, incompressible, steady, fully developed and turbulent.
2. There is a negligible change in thermo-physical properties of air and absorber plate for the operating range of temperatures and hence can be assumed to be constant.
3. The material of duct wall, absorber plate and artificial roughness are homogeneous and isotropic.
4. All the walls in contact with the fluid are assigned no-slip boundary condition.
5. Heat loss in form of radiation is negligible.

III. Data Reduction

The results obtained by CFD simulation of solar air heater has to be compare with that of the smooth duct in order to find out the enhancement in performance. The Nusselt number and friction factor for the smooth duct (Nu_s and f_s) can be obtained using Dittus-Boelter Equation [23] and Modified Blasius Equation [24] respectively.

$$\text{Dittus-Boelter Equation: } Nu_s = 0.023\,\mathrm{Re}^{0.8}\,\mathrm{Pr}^{0.4} \quad (1)$$

$$\text{Modified Blasius Equation: } f_s = 0.085\,\mathrm{Re}^{-0.25} \quad (2)$$

The average velocity *v* for a particular value of Reynolds number can be calculated using the equation

$$v = \frac{\mu(\mathrm{Re})}{\rho D_H} \quad (3)$$

After obtaining the value of '*h'* from the simulation of roughened duct we can find out numerical value of Average Nusselt Number using equation

$$Nu = \frac{hD_H}{k} \tag{4}$$

After obtaining the value of '$\Delta P / l$' from the simulation of smooth as well as roughened duct we can find out numerical value of Average Friction Factor using equation

$$f = \frac{(\Delta P / l)D_H}{2\rho v^2} \tag{5}$$

where $\Delta P / l$ = Pressure Drop per unit length of the duct

Introduction of artificial roughness enhances both Nusselt number as well as friction factor. Although enhancement in Nusselt number is desirable while enhancement in friction factor is undesirable since it leads to high pumping power requirement. Hence a parameter is defined for studying the overall performance of solar air heater namely Thermo Hydraulic Performance Parameter (THPP). It is computed by

$$THPP = \frac{Nu_r / Nu_s}{(f_r / f_s)^{1/3}} \tag{6}$$

For the feasibility of the artificial roughness THPP should always be greater than unity.

For studying the overall performance of solar air heater having particular geometry of duct, the mean value of performance parameters like Nusselt Number Ratio (Nu_r/Nu_s), Friction Factor Ratio (f_r/f_s) and Thermo Hydraulic performance parameter can be evaluated and compared for the range of operating velocity (Reynolds Number). It can be computed as

$$\text{Mean THPP} = \frac{[(\text{THPP})_{@Re=3000} + (\text{THPP})_{@Re=6000} + \ldots\ldots\ldots\ldots + (\text{THPP})_{@\ Re\ =\ 18000}]}{6} \tag{7}$$

Similarly Mean (Nu_r/Nu_s) and Mean (f_r/f_s) can also be evaluated for each roughened geometry. Among the various roughened geometries simulated the geometry with maximum value of Mean THPP will give the best performance for the selected range of Reynolds Number (Re = 3000 to Re = 18,000).

IV. Results and Discussion

A. Selection and Validation of Turbulence Model

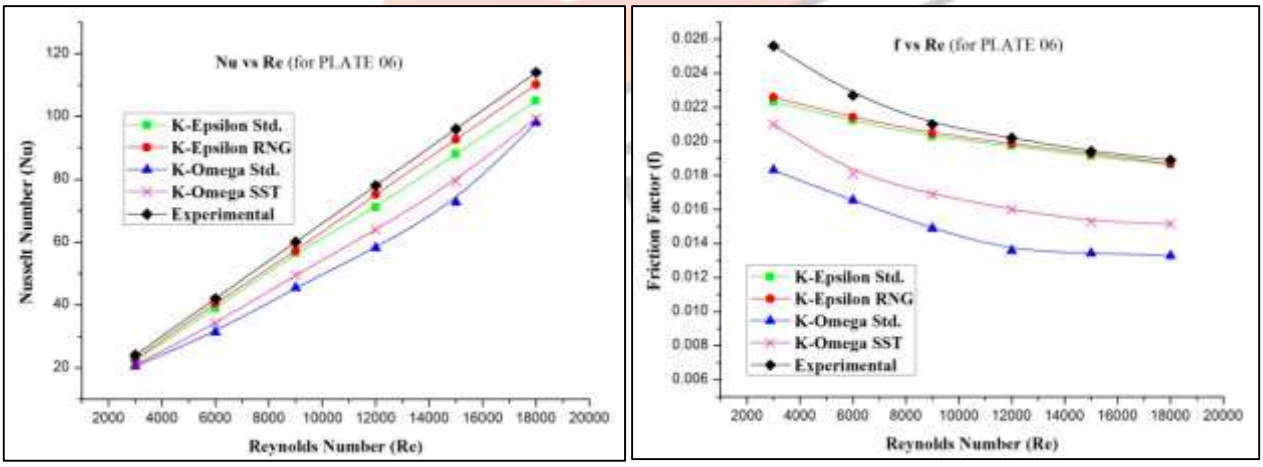

figure 4: variation of (a) nusselt number and (b) friction factor with reynolds number for plate 06 using various turbulence models

In the present study the duct width, duct height and aspect ratio of duct are kept same as that of experimental investigation conducted by Layek et al [20].In both the cases duct width is 150mm, duct height is 30mm and aspect ratio is 5. Hence the result available from experimental investigation of 0° chamfer ribs (square ribs) can be used for the selection of appropriate turbulence model. Among the 16 different absorber plate geometries, Plate 06 is having same dimensions to that considered in experimental investigation. Hence numerical simulation for Plate 06 is carried out using K-ϵ Standard, K-ϵ RNG, K-ω Standard and K-ω SST turbulence models.

Figure 4(a) and 4(b) shows variation of Nusselt Number and Friction Factor with Reynolds Number for Plate 06 for various turbulence models. It is quite clear from the diagram that results obtained using K-ϵ Standard and K-ϵ RNG are in good agreement with the experimental results available while K-ω Standard and K-ω SST gives comparatively poor results. Among all

the models K-ω Standard gives worst result while K-ϵ RNG gives best results. Also the review of literature of numerical simulation of solar air heater [2] and [4] reveals that in majority of the numerical investigations K-ϵ RNG is found to be most suitable. Hence K-ϵ RNG model is selected for further simulation of solar air heater for various geometries of absorber plates. The Average % deviation in numerical values of Nu and f from experimental values are ± 4.28 % and ± 3.92% respectively.

B. Heat Transfer in Roughened duct

The introduction of artificial roughness in the form of compound turbulators on the absorber plate considerably increases the heat transfer and flow characteristics inside the duct. The variation in heat transfer with variation in Relative Roughness Height (e/D_H) and Relative Roughness Pitch (P/e) are plotted for the range of Reynolds Number to study the effect of relative roughness height on thermal performance. Also the streamlines merged with contours of turbulent kinetic energy is also drawn in order to physically understand the variation of flow with variation in relative roughness height.

1. Effect of Relative Roughness Height (e/D_H) on Heat Transfer

Figure 5 (a), (b), (c) and (d) shows variation in Nu with change in Re for various e/D_H and at constant P/e. All the values shown in Figure 5(a) corresponds to P/e =8. Similarly all the values in Figure 5(b), 5(c) and 5(d) corresponds to P/e = 10, 12 and 15 respectively. It is observed that for all the four cases Nu increases with increase in Re. It is well known that increase in Reynolds number increases turbulent kinetic energy and turbulent dissipation rate, which leads to increase in the turbulent intensity and thus increases the Nusselt number. Also for all P/e the highest Nu is obtained for e/D_H = 0.040 which is indicated by pink cross in all graphs. The highest value of Nu obtained is 140.1690 corresponding to Plate 14 (P/e =10 and e/D_H = 0.040).

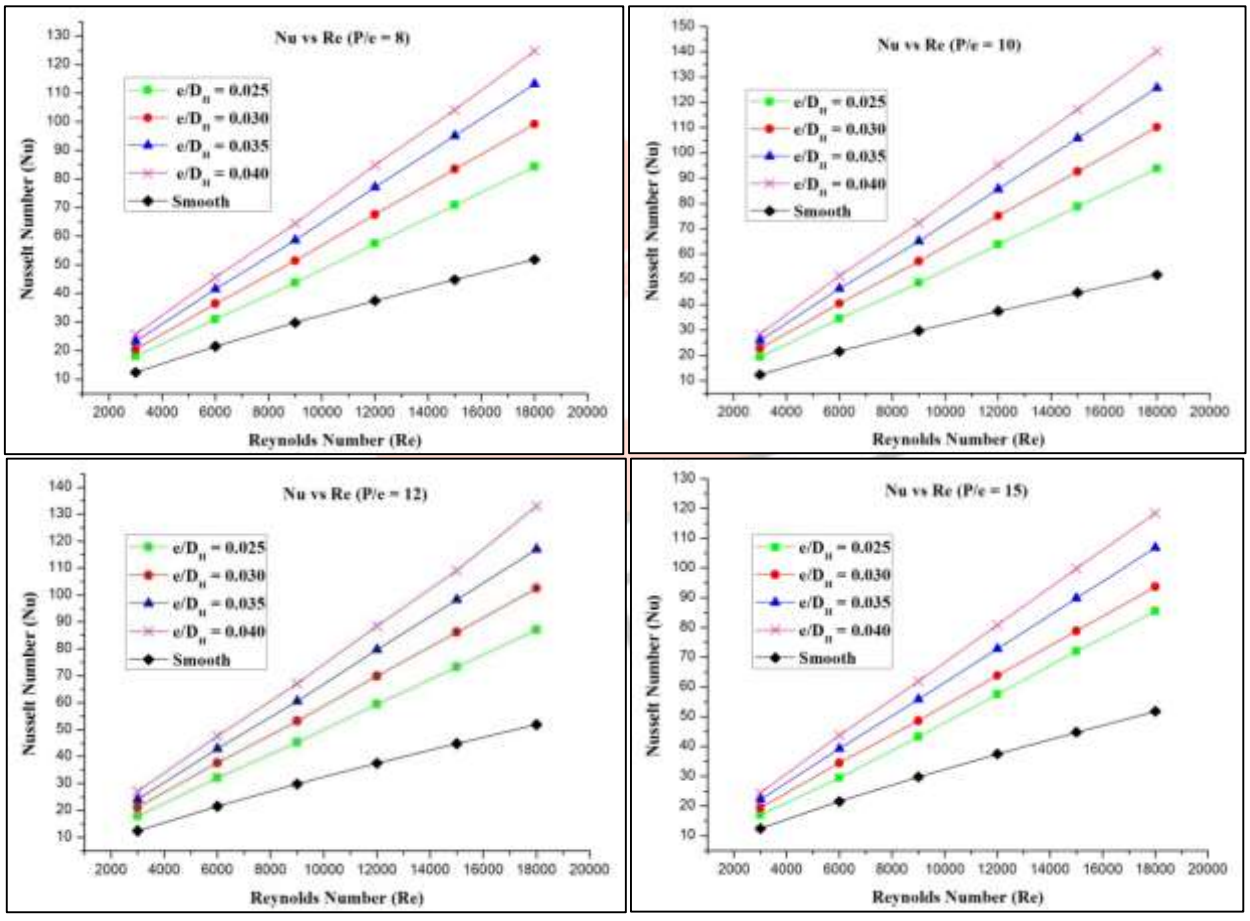

figure 5: variation of nusselt number with reynolds number at different values of relative roughness height (e/D_H) at a) P/e = 8 b) P/e = 10 c) P/e = 12 d) P/e = 15

Figure 6 (a), (b), (c) and (d) shows variation in Nu with change in P/e for various Re and at constant e/D_H. All the values shown in Figure 6(a) corresponds to P/e =8. Similarly all the values in Figure 6(b), 6(c) and 6(d) corresponds to P/e = 10, 12 and 15 respectively. It is observed that for all the four cases Nu increases with increase in e/D_H and is highest at e/D_H = 0.040. The increase in Nu with increase in e/D_H is due to the fact that higher e/D_H creates turbulence in comparatively larger area which leads to higher turbulent kinetic energy, more uniform distribution of heat and hence higher convective heat transfer coefficient.

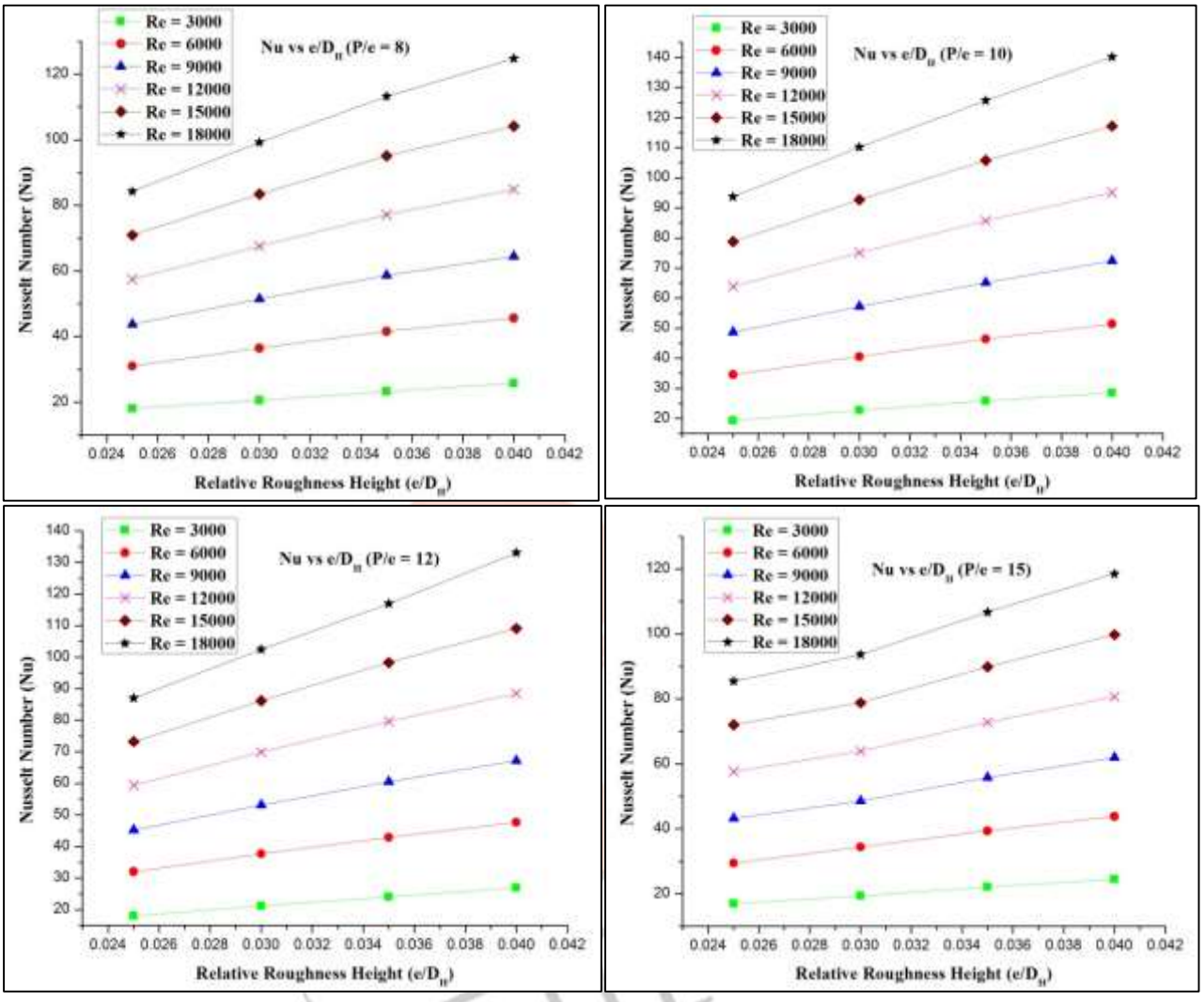

figure 6: variation of nusselt number with relative roughness height (e/D_H) at different values of reynolds number at a) P/e = 8 b) P/e = 10 c) P/e = 12 d) P/e = 15

Figure 7 (a), (b), (c) and (d) shows variation in flow pattern with variation in e/D_H at P/e =10. Streamlines are overlapped with the contours of turbulent kinetic energy to understand the effect of flow pattern on the turbulence at the inter rib region. In all the four cases the turbulent kinetic energy is high near the inter rib region where vortices are generated. Also it can be concluded from above four figures that for constant relative roughness pitch the flow pattern remains almost identical. The only difference is in the size of the vortices formed adjacent to the ribs. Higher relative roughness height leads to larger size of vortices which increases the area affected by the ribs inside the duct and hence enhancement in turbulent kinetic energy (refer values indicated in scale) and heat transfer rate is obtained.

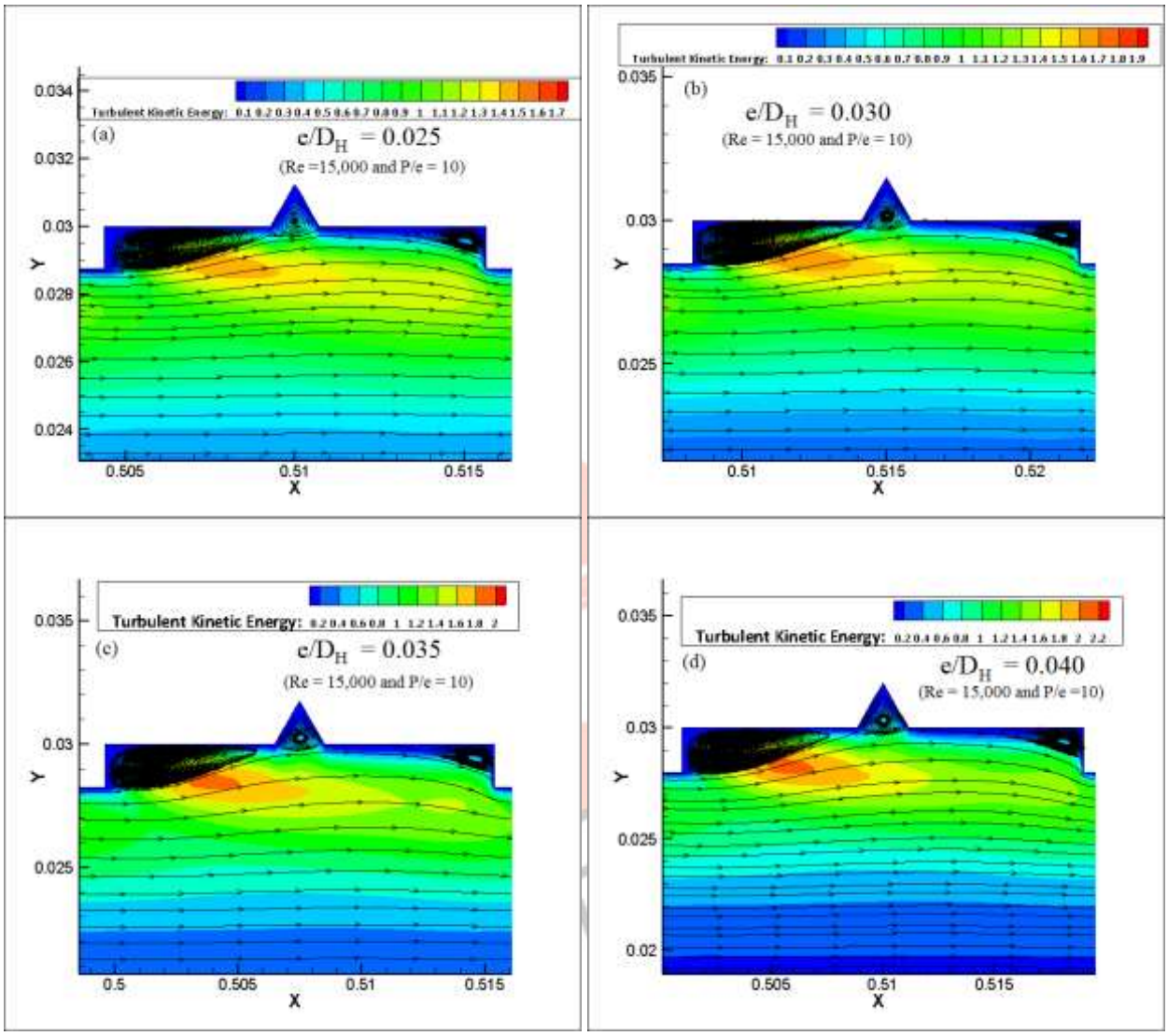

figure:7 Streamlines for Re = 15,000 and at P/e = 10 (a) $e/D_H = 0.025$ (b) $e/D_H = 0.030$ (c) $e/D_H = 0.035$ (d) $e/D_H = 0.040$

2. Effect of Relative Roughness Pitch (P/e) on Heat Transfer

Figure 8 (a), (b), (c) and (d) shows variation in Nu with change in Re for various P/e and at constant $e/D_{H.}$ All the values shown in Figure 8(a) corresponds to e/D_H = 0.025. Similarly all the values in Figure 8(b), 8(c) and 8(d) corresponds to e/D_H = 0.030, 0.035 and 0.040 respectively. It is observed that for all the four cases there is an increment in Nu with increment in Re. It is well known that increase in Reynolds number increases turbulent kinetic energy and turbulent dissipation rate, which leads to increase in the turbulent intensity and thus increases the Nusselt number. For all the combinations of P/e and $e/D_{H,}$ Nu obtained is higher to that of Smooth duct for same Re. Also for all e/D_H the highest Nu is obtained for P/e =10 which is indicated by red dot in all graphs. The highest value of Nu obtained is 140.1690 corresponding to P/e =10 and e/D_H = 0.040.

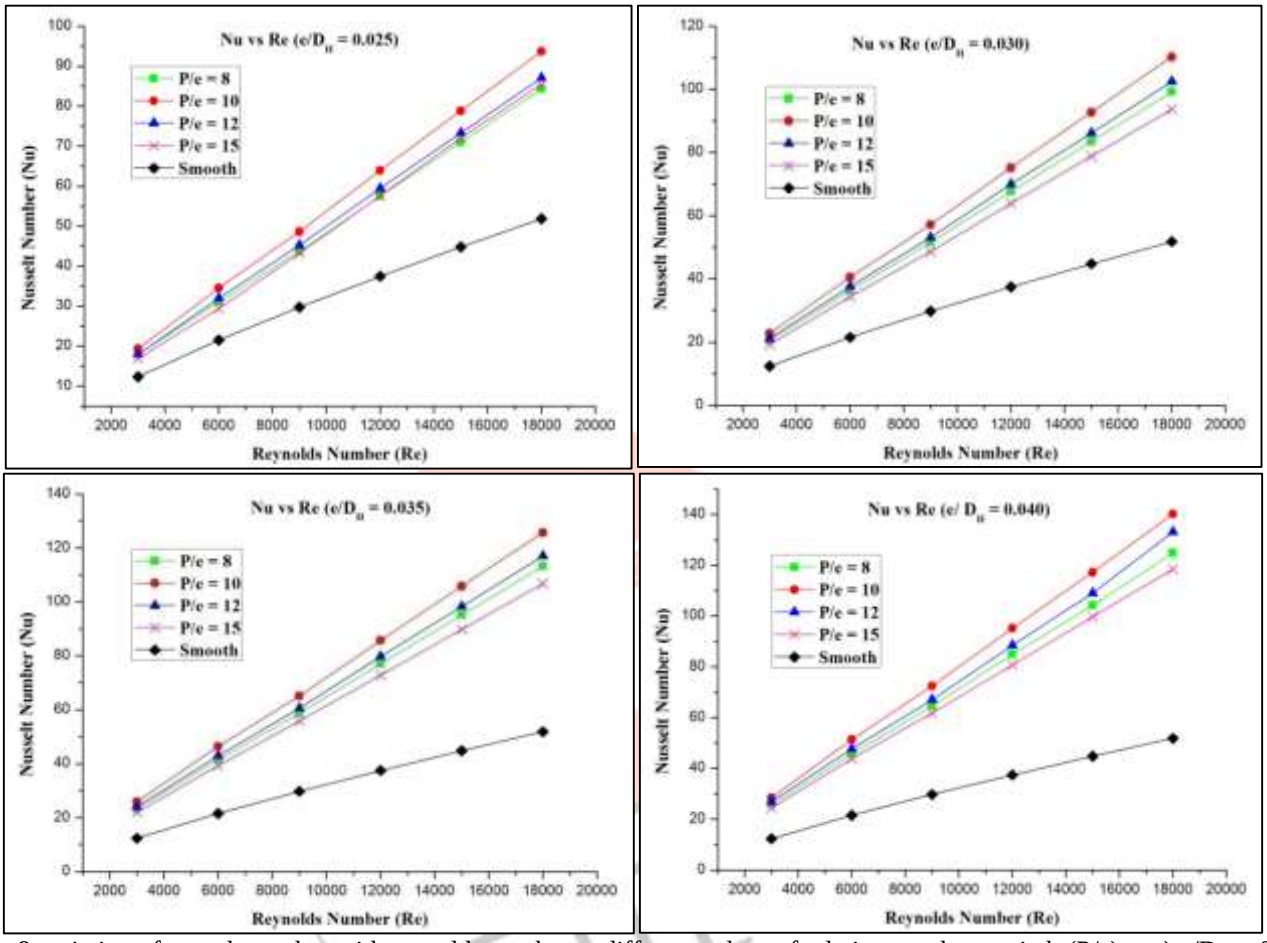

figure:8 variation of nusselt number with reynolds number at different values of relative roughness pitch (P/e) at a) e/D_H = 0.025 b) e/D_H = 0.030 c) e/D_H = 0.035 d) e/D_H = 0.040

Figure 9 (a), (b), (c) and (d) shows variation in Nu with change in P/e for various Re and at constant e/D_H. All the values shown in Figure 9(a) corresponds to e/D_H = 0.025. Similarly all the values in Figure 9(b), 9(c) and 9(d) corresponds to e/D_H = 0.030, 0.035 and 0.040 respectively. It is observed that for all the four cases, with increase in P/e, Nu first increases from P/e = 8 to P/e = 10 where it is maximum, then it decreases from P/e = 10 to P/e =12 and then it further decreases from P/e =12 to P/e =15. The reason of getting highest Nu at P/e = 10 is discussed in the later subsection of this chapter where streamlines and flow patterns are discussed. Also the difference in the values of Nu at various P/e is very low for lower velocity (Re=3000), but this difference slowly increases with increase in Re.

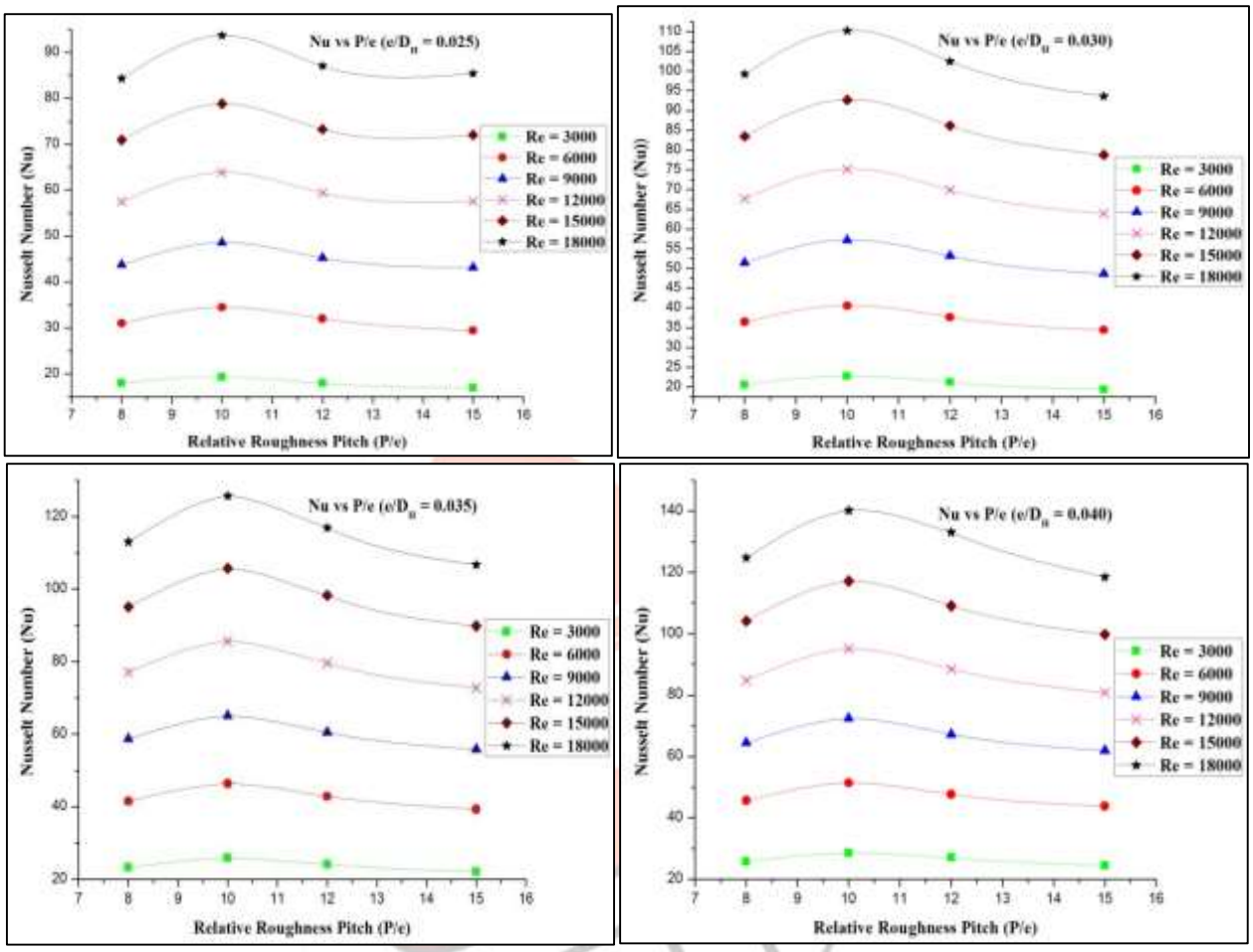

figure:9 variation of nusselt number with relative roughness pitch (P/e) at different values of reynolds number at a) e/D_H = 0.025 b) e/D_H = 0.030 c) e/D_H = 0.035 d) e/D_H = 0.040

Figure 10(a), (b), (c) and (d) shows variation in flow pattern with variation in P/e at e/D_H =0.040. In all four cases vortices are formed adjacent to the ribs and at the groove. For relative roughness pitch P/e = 8 reattachment will not occur, which results in the decrease of the heat enhancement rate. When the relative roughness pitch is increased (P/e =10) reattachment will occur which results in higher heat enhancement rate. When the P/e is increased further to 12 and 15 separation and reattachment of flow occurs, but due to more length as compared to that in case of P/e =10 the effect of vortices formation will decrease and slowly becomes negligible which will be clearly indicated by the contour of turbulent kinetic energy. Thus flow separation further downstream will results in decrease of heat enhancement rate beyond roughness pitch P/e =10.

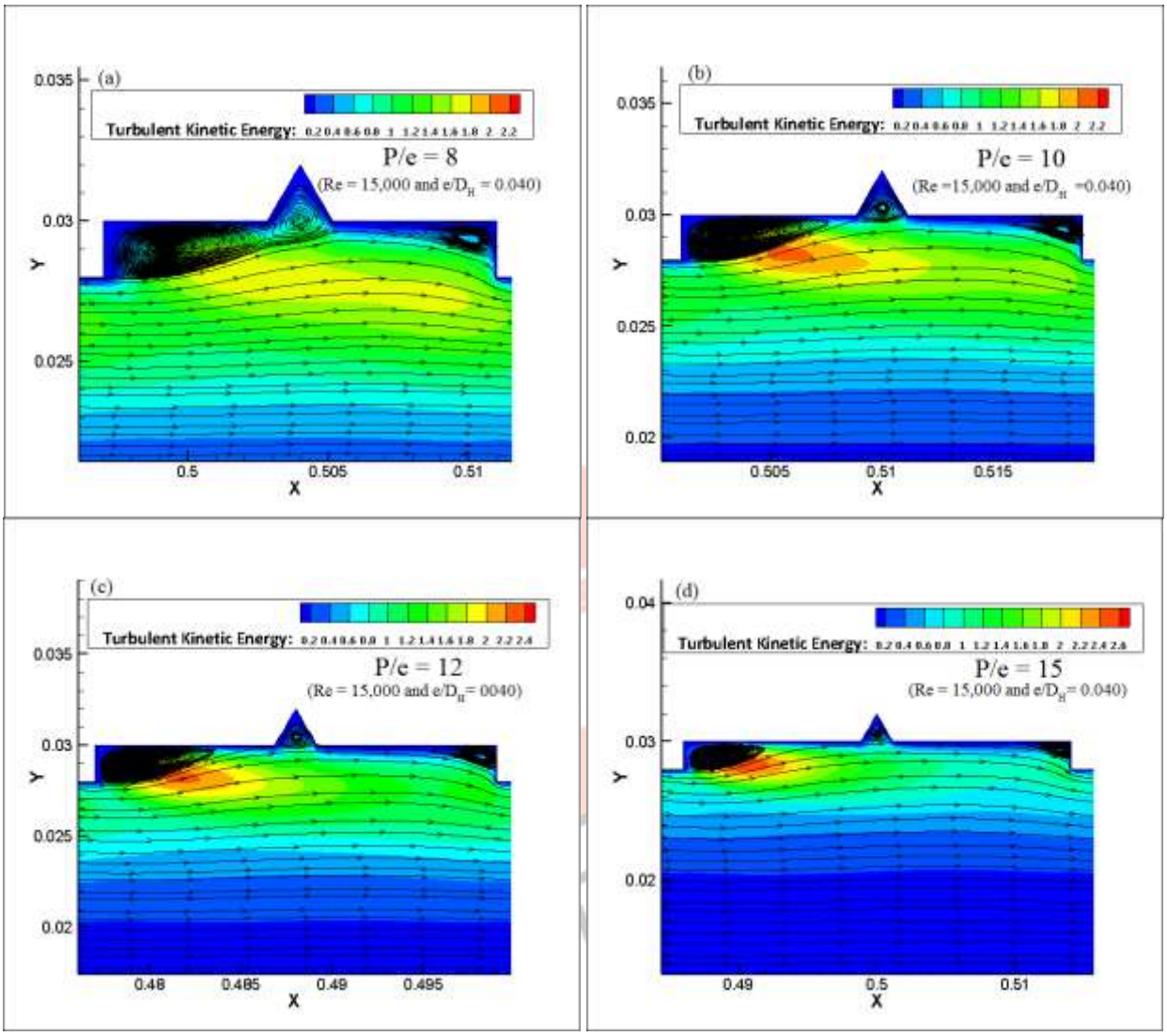

figure:10 streamlines for Re = 15,000 and e/D_H =0.040 at (a) P/e = 8 (b) P/e = 10 (c) P/e =12 (d) P/e =15

C. Friction Factor in Roughened duct

The variation in friction factor with variation in Relative Roughness Height (e/D_H) and Relative Roughness Pitch (P/e) are plotted for the range of Reynolds Number to study the effect of relative roughness height on thermal performance. Also the streamlines merged with contours of turbulent kinetic energy is also drawn in order to physically understand the variation of flow with variation in relative roughness height.

1. Effect of Relative Roughness Height (e/D_H) on Friction Factor

Figure 11 (a), (b), (c) and (d) shows variation in f with change in Re for various e/D_H and at constant P/e. All the values shown in Figure 11(a) corresponds to P/e =8. Similarly all the values in Figure 11(b), 11(c) and 11(d) corresponds to P/e = 10, 12 and 15 respectively. It is observed that for all the four cases f decreases with increase in Re which is due to the fact that for low velocity or low Re viscous forces dominates over the inertia forces which provides resistance to the flow of air and hence friction factor is high. Also for all P/e the highest f is obtained for $e/D_H = 0.040$ which is indicated by pink cross in all graphs. The highest value of f obtained is 0.0278 corresponding to Plate 13 (P/e =15 and $e/D_H = 0.040$).

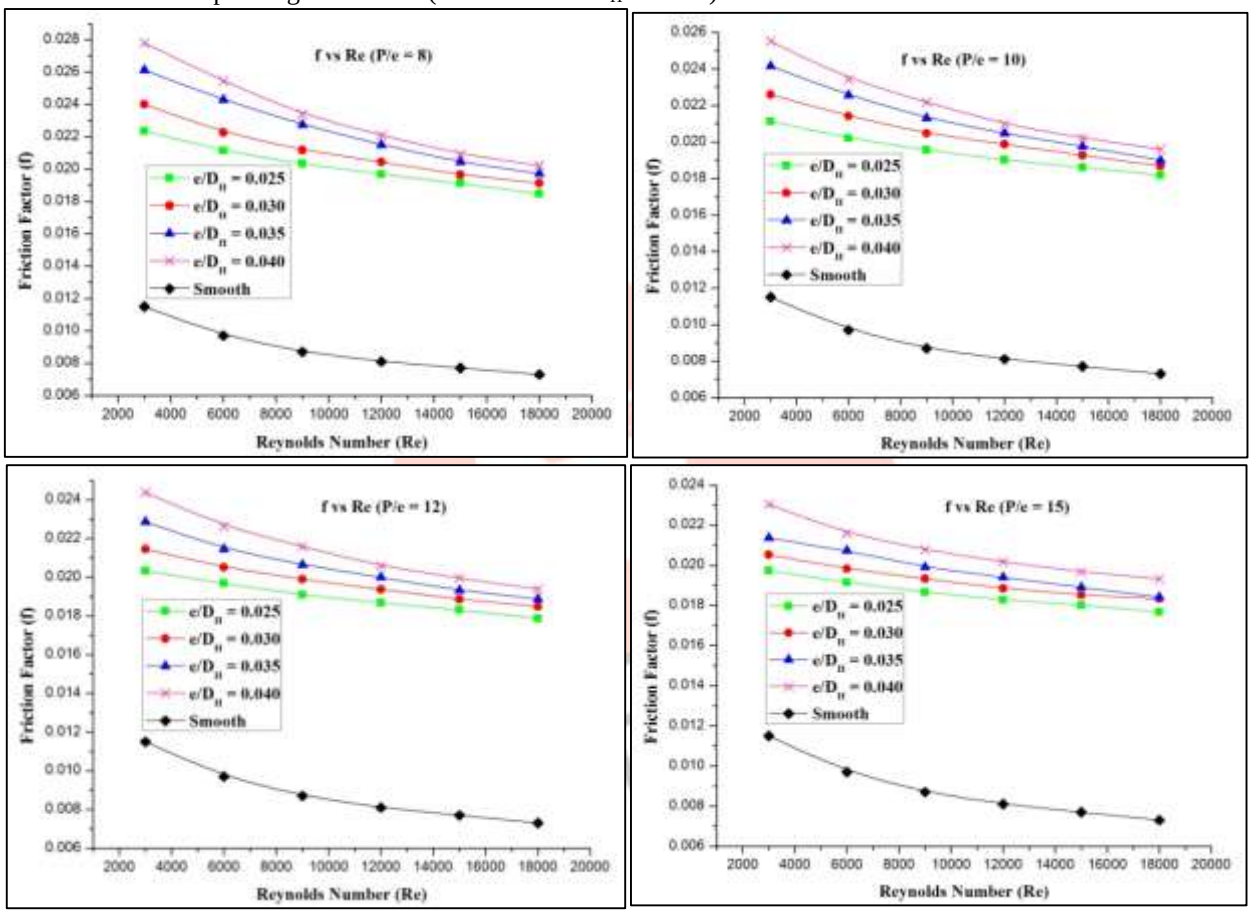

figure:11 variation of friction factor with reynolds number at different values of relative roughness height (e/D_H) at a) P/e = 8 b) P/e = 10 c) P/e = 12 d) P/e = 15

Figure 12 (a), (b), (c) and (d) shows variation in f with change in P/e for various Re and at constant e/D_H. All the values shown in Figure 12(a) corresponds to P/e =8. Similarly all the values in Figure 12(b), 12(c) and 12(d) corresponds to P/e = 10, 12 and 15 respectively. It is observed that for all the four cases f increases with increase in e/D_H and is highest at e/D_H = 0.040. The increase in f with increase in e/D_H is due to the fact that higher e/D_H provides obstruction in comparatively larger area which leads to higher pressure drop hence higher friction factor.

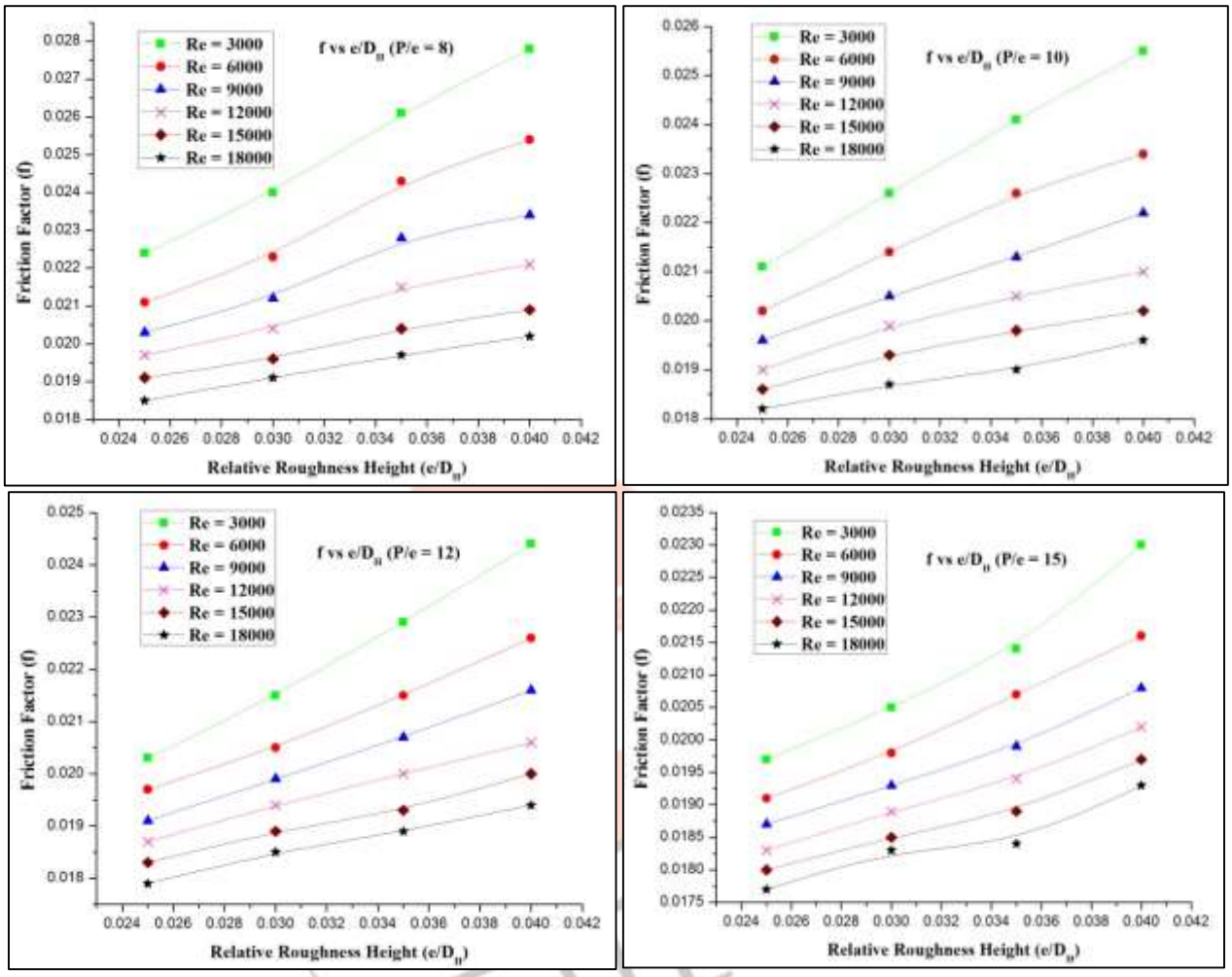

figure:12 variation of friction factor with relative roughness height (e/D_H) at different values of reynolds number at a) P/e = 8 b) P/e = 10 c) P/e = 12 d) P/e = 15

Figure 13 (a), (b), (c) and (d) shows variation in f with change in Re for various P/e and at constant e/D_H. All the values shown in Figure 13(a) corresponds to $e/D_H = 0.025$. Similarly all the values in Figure 13(b), 13(c) and 13(d) corresponds to $e/D_H = 0.030$, 0.035 and 0.040 respectively. It is observed that for all the four cases there is a decrement in f with increment in Re. The decrement in f with increment in Re is due to the fact that for low velocity or low Re viscous forces dominates over the inertia forces which provides resistance to the flow of air and hence friction factor is high. . For all the combinations of P/e and e/D_H, f obtained is higher to that of Smooth duct for same Re. Also for all e/D_H the highest Nu is obtained for P/e =8 which is indicated by green square in all graphs. The highest value of f obtained is 0.0278 corresponding to Plate 13 (P/e = 8 and $e/D_H = 0.040$).

2. Effect of Relative Roughness Pitch (P/e) on Friction Factor

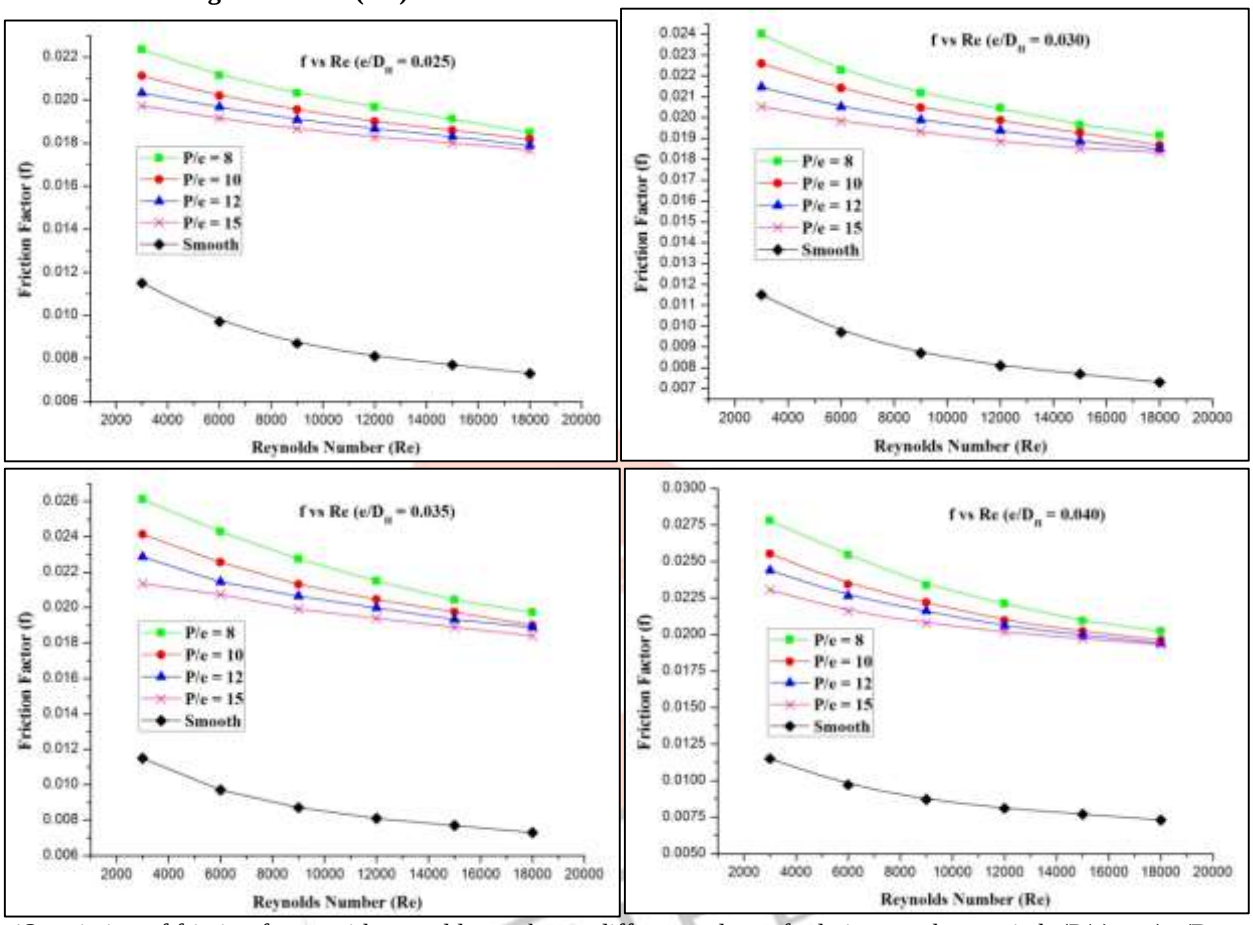

figure:13 variation of friction factor with reynolds number at different values of relative roughness pitch (P/e) at a) $e/D_H = 0.025$ b) $e/D_H = 0.030$ c) $e/D_H = 0.035$ d) $e/D_H = 0.040$

Figure 14 (a), (b), (c) and (d) shows variation in f with change in P/e for various Re and at constant e/D_H. All the values shown in Figure 14(a) corresponds to $e/D_H = 0.025$. Similarly all the values in Figure 14(b), 14(c) and 14(d) corresponds to $e/D_H = 0.030$, 0.035 and 0.040 respectively. It is observed that for all the four cases, there is a decrement in f with increment in P/e. The reason of getting higher Nu at P/e = 8 is due to the fact that absorber plate having lower P/e would have more number of ribs for the same length of the duct. More number of ribs per unit length leads to more resistance to the flow of air which leads to higher pressure drop and hence higher friction factor. Also the difference in the values of f at various P/e is very low for higher velocity (Re=18000), but this difference slowly increases with decrease in Re.

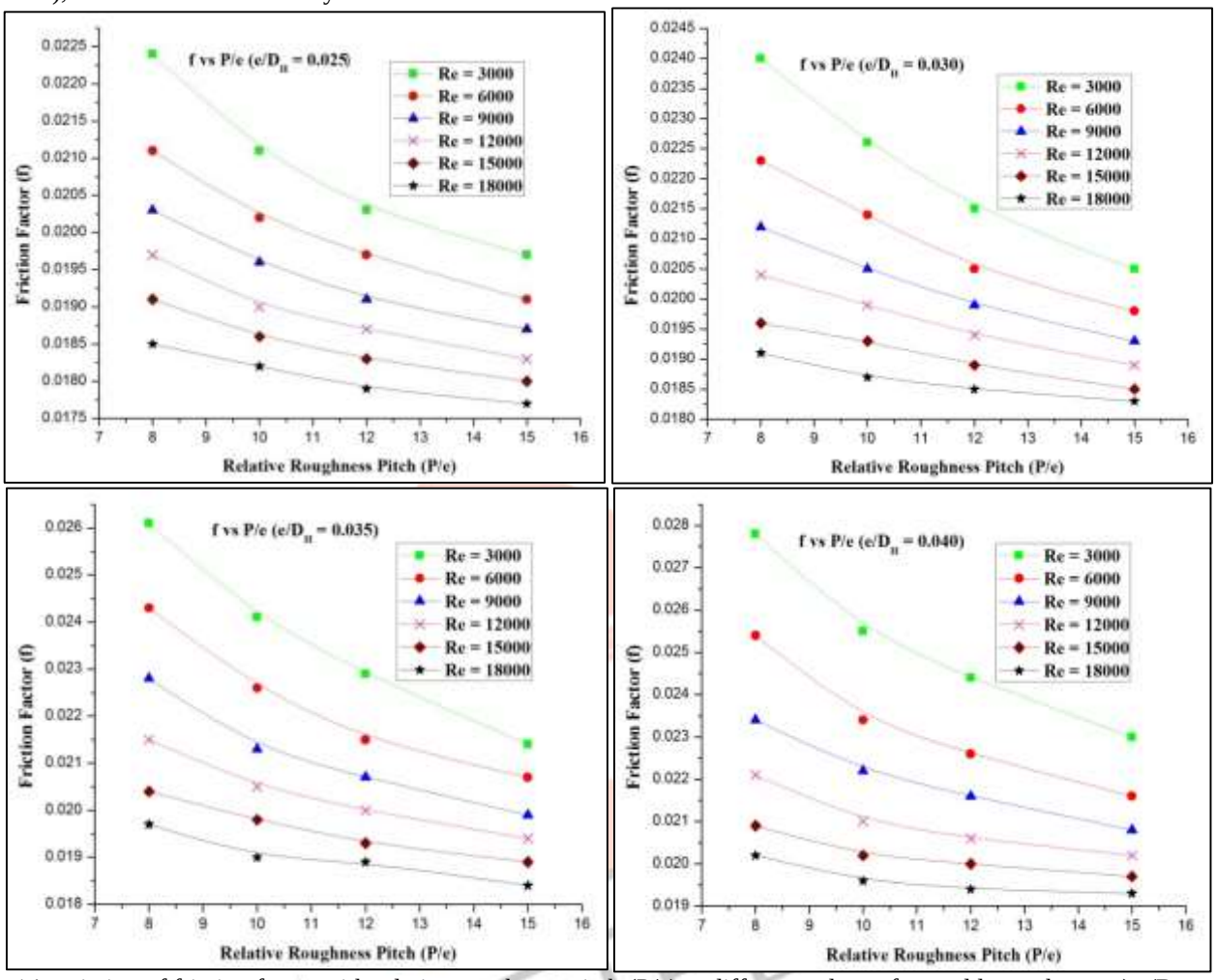

figure:14 variation of friction factor with relative roughness pitch (P/e) at different values of reynolds number at a) $e/D_H = 0.025$ b) $e/D_H = 0.030$ c) $e/D_H = 0.035$ d) $e/D_H = 0.040$

D. Performance Parameters

1. Mean Nusselt Number Ratio (Nu_r / Nu_s)

For all sixteen geometries of absorber plates there is an increment in Nu_r/Nu_s ratio with increment in Re. So instead of showing its variation with Re a mean value of Nusselt Number ratio is evaluated for each absorber plate for the range of Re = 3000 to Re =18,000 and then the variation in Mean Nu_r/Nu_s is studied with variation in P/e at each e/D_H. Figure 15 shows Variation in Mean Nusselt Number Ratio (Nu_r/Nu_s) with change in P/e at various e/D_H. It is quite clear that Mean Nu_r/Nu_s increases with increase in e/D_H. With increase in P/e, Nu_r/Nu_s first increases from P/e = 8 to P/e = 10 where it is maximum, then it decreases from P/e = 10 to P/e =12 and then it further decreases from P/e =12 to P/e =15.

The highest Mean Nu_r/Nu_s ratio comes out to be 2.4979 for Plate 14 (P/e = 10, e/D_H = 0.040).

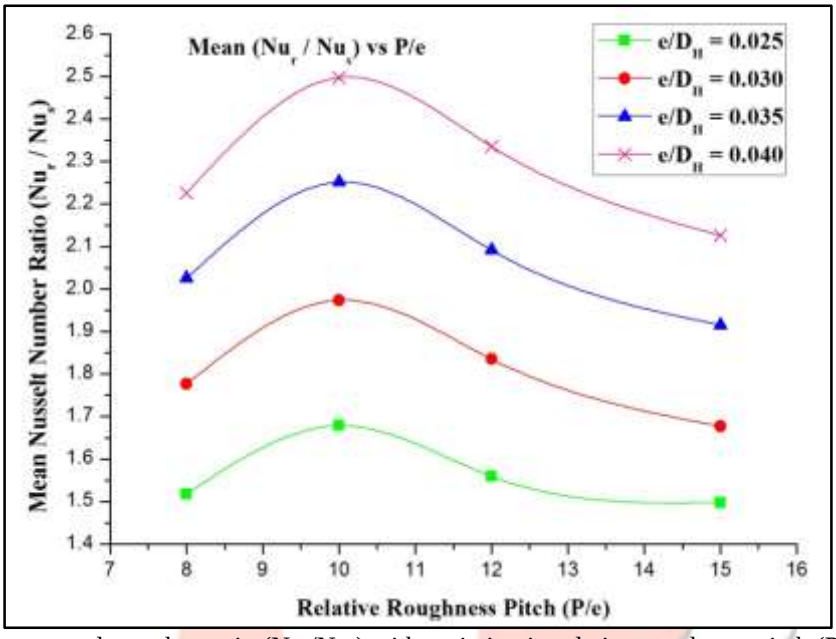

figure:15 variation in mean nusselt number ratio (Nu_r/Nu_s) with variation in relative roughness pitch (P/e) at different values of e/D_H

2. Mean Friction Factor Ratio (f_r / f_s)

Like Nu_r / Nu_s for all sixteen geometries of absorber plates there is an increment in f_r/f_s ratio with increment in Re. So instead of showing its variation with Re a mean value of friction factor ratio is evaluated for each absorber plate for the range of Re = 3000 to Re =18,000 and then the variation in Mean f_r/f_s is studied with variation in P/e at each e/D_H. Figure 16 shows Variation in Mean Friction Factor Ratio (f_r/f_s) with change in P/e at various e/D_H. It is quite clear that Mean f_r/f_s increases with increase in e/D_H and f_r/f_s decreases with increase in P/e. The highest Mean f_r/f_s ratio comes out to be 2.6573 for Plate 13 (P/e = 8, e/D_H = 0.040).

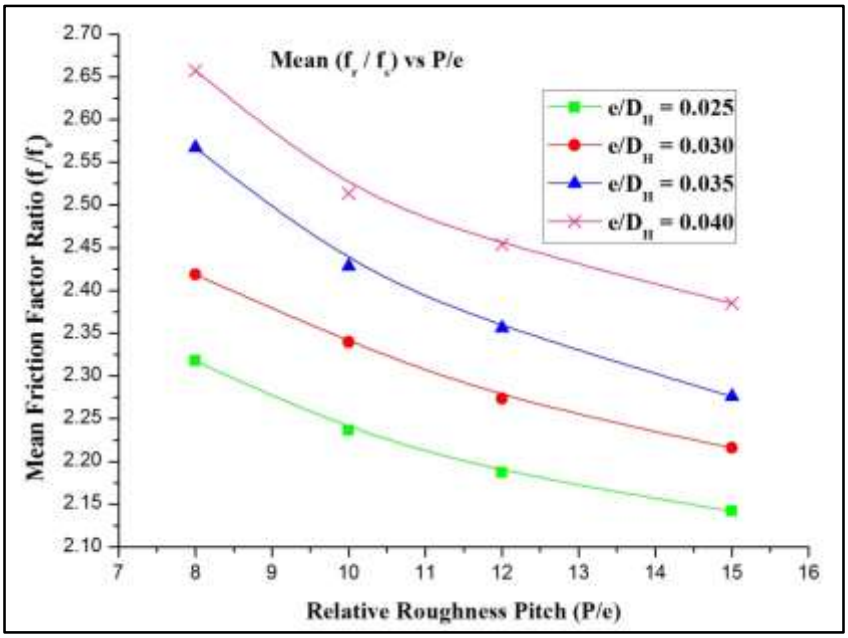

figure:16 variation in mean friction factor ratio (f_r/f_s) with variation in relative roughness pitch (P/e) at different values of e/D_H

3. Mean Thermo Hydraulic Performance Parameter (THPP)

THPP is evaluated using equation (6) for all the geometries of an absorber plate and at each Reynolds Number. The highest value of THPP obtained is 1.9456 (corresponding to Re =18,000, e/D_H = 0.040 and P/e = 10) which is greater to that of highest THPP = 1.87 obtained by numerical simulation of transverse square ribs by Anil Singh Yadav, J.L.Bhagoria [16]. The value of THPP not only varies with respect to geometry of an absorber plate but also it varies with variation in Reynolds Number (generally it increases with increase in Re). So in order to select the best suitable geometry a mean value of THPP is evaluated using equation (7) for each absorber plate for the range of Re = 3000 to Re =18,000 and then the Mean THPP is studied with change in P/e at each e/D_H. This Mean THPP indicates the overall performance of solar air heater for particular geometry of an absorber plate for the range of velocity (Re = 3000 to Re = 18,000). Figure 17 shows Variation in Mean THPP with change in P/e at various e/D_H. It is quite clear that Mean THPP increases with increase in e/D_H. With increase in P/e, THPP first increases from P/e = 8 to P/e = 10 where it is maximum, then it decreases from P/e = 10 to P/e =12 and then it further decreases from P/e =12 to P/e =15. The highest Mean THPP comes out to be 1.8369 for Plate 14 (P/e = 10, e/D_H = 0.040).

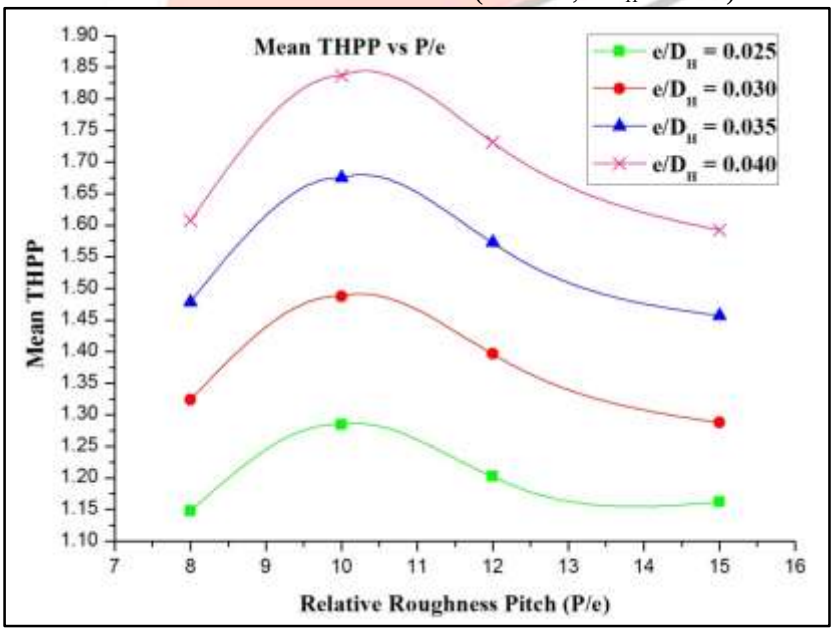

figure:17 variation in mean thermo hydraulic performance parameter (THPP) with variation in relative roughness pitch (P/e) at different values of e/D_H

V. CONCLUSIONS

A numerical study of the flow of air in a rectangular duct with one roughened wall subjected to uniform heat flux and with the other three smooth walls being insulated has been performed. These conditions correspond to the flow in the duct of a solar air

heater. The effect of relative roughness pitch, relative roughness height at constant relative groove position on the friction factor and heat transfer coefficient has been studied.

The major conclusions are:

1) As compared to the smooth duct, the introduction of compound turbulators yields Nusselt number from 1.3668 to 2.7041 times while the friction factor rises from 1.7162 to 2.7711 times for the range of parameters investigated.

2) The maximum heat transfer occurs for a relative roughness pitch of 10, while the friction factor goes on decreasing as the relative roughness pitch increases.

3) Both heat transfer and friction factor goes on increasing with increase in relative roughness height for the range of parameters investigated.

4) For selected range of roughness parameter, the range of the Thermo Hydraulic Performance Parameter for the roughened duct with compound turbulators comes out to be 1.0896 to 1.9456. The highest THPP obtained (1.9456) is greater to that of highest THPP (1.87) obtained by numerical simulation of transverse square ribs by Anil Singh Yadav, J.L.Bhagoria [16]

5) The Mean THPP for the range of Re = 3000 to 18,000 is maximum (1.8369) for Plate 14. Hence Plate 14 (P/e = 10 and e/D_H = 0.040) has an optimized geometry of absorber plate for the range of roughness parameter investigated.

VI. REFERENCES

[1] Kumar A, Saini RP, Saini JS. Heat and fluid flow characteristics of roughened solar air heater ducts - A review. Renewable Energy 47 (2012) 77-94.
[2] Yadav AS, Bhagoria JL. Heat transfer and fluid flow analysis of solar air heater: A review of CFD approach. Renewable and Sustainable Energy Reviews 23 (2013) 60–79.
[3] Sharma SK, Kalamkar VR. Thermo-hydraulic performance analysis of solar air heaters having artificial roughness- A review. Renewable and Sustainable Energy Reviews 41 (2015) 413–435.
[4] Sharma SK, Kalamkar VR. Computational Fluid Dynamics approach in thermo-hydraulic analysis of flow in ducts with rib roughened walls – A review. Renewable and Sustainable Energy Reviews 55 (2016) 756-788.
[5] Bhagoria JL, Saini JS, Solanki SC. Heat transfer coefficient and friction factor correlations for rectangular solar air heater duct having transverse wedge shaped rib roughness on the absorber plate. Renewable Energy 25 (2002) 341–369.
[6] Chaube A, Sahoo PK, Solanki SC. Analysis of heat transfer augmentation and flow characteristics due to rib roughness over absorber plate of a solar air heater. Renewable Energy 31 (2006) 317–331.
[7] Aharwal KR, Gandhi BK, Saini JS. Experimental investigation on heat- transfer enhancement due to a gap in an inclined continuous rib arrangement in a rectangular duct of solar air heater. Renewable Energy 33 (2008) 585–596.
[8] Saini SK, Saini RP. Development of correlations for Nusselt number and friction factor for solar air heater with roughened duct having arc- shaped wire as artificial roughness. Solar energy 82 (2008) 1118–1130.
[9] Kumar A, Bhagoria JL, Sarviya RM. Heat transfer and friction correlations for artificially roughened solar air heater duct with discrete W-shaped ribs. Energy Conversion and Management 50 (2009) 2106–2117.
[10] Lanjewar A, Bhagoria JL, Sarviya RM. Experimental study of augmented heat transfer and friction in solar air heater with different orientations of W- rib roughness. Experimental Thermal and Fluid Science 35 (2011) 986–995.
[11] Lanjewar A, Bhagoria JL, Sarviya RM. Heat transfer and friction in solar air heater duct with W-shaped rib roughness on absorber plate. Energy 36 (2011) 4531-4541.
[12] Kumar A, Saini RP, Saini JS. Experimental investigation on heat transfer and fluid flow characteristics of air flow in a rectangular duct with Multi v- shaped rib with gap roughness on the heated plate. Solar Energy 86 (2012) 1733–1749.
[13]Kumar S, Saini RP. CFD based performance analysis of a solar air heater duct provided with artificial roughness. Renewable Energy 34 (2009) 1285–1291.
[14] Karmare SV and Tikekar AN. Analysis of fluid flow and heat transfer in a rib grit roughened surface solar air heater using CFD. Solar Energy 84 (2010) 409–417.
[15] Yadav AS, Bhagoria JL. A CFD (computational fluid dynamics) based heat transfer and fluid flow analysis of a solar air heater provided with circular transverse wire rib roughness on the absorber plate. Energy 55 (2013) 1127-1142.
[16] Yadav AS, Bhagoria JL. A numerical investigation of square sectioned transverse rib roughened solar air heater. International Journal of Thermal Sciences 79 (2014) 111-131.
[17] Yadav AS, Bhagoria JL. A CFD based thermo-hydraulic performance analysis of an artificially roughened solar air heater having equilateral triangular sectioned rib roughness on the absorber plate. International Journal of Heat and Mass Transfer 70 (2014) 1016–1039.
[18] Boukadoum AB, Benzaoui A. CFD based analysis of heat transfer enhancement in solar air heater provided with transverse rectangular ribs. Energy Procedia 50 (2014) 761 – 772.
[19] Jin D, Zhang M, Wang P, Xu S. Numerical investigation of heat transfer and fluid flow in a solar air heater duct with multi V-shaped ribs on the absorber plate. Energy 89 (2015) 178-190.

[20] Layek A, Saini JS, Solanki SC. Effect of chamfering on heat transfer and friction characteristics of solar air heater having absorber plate roughened with compound turbulators. Renewable Energy 34 (2009) 1292–1298.
[21] ASHARE Standard 93-97. Method of testing to determine the thermal performance of solar collectors, 1977.
[22] www.cfd-online.com/Tools/yplus.php
[23] McAdams WH (1942) Heat Transmission. McGraw-Hill, New York.
[24] Kays W.M., Perkin H. Forced convection internal flow in ducts. In: Rohsenow W.M., Hartnett I.V., editors, Handbook of Heat Transfer. New York: McGraw-Hill.